Topological and Geometric Properties of Interval Solid Models

T. Sakkalis, G. Shen and N. M. Patrikalakis

Massachusetts Institute of Technology

Cambridge, MA 02139–4307, USA

Design Laboratory Memorandum 99-6

Copyright ©2000 Massachusetts Institute of Technology

All rights reserved

November 19, 1999

Revised: October 27, 2000

Abstract

A solid is a connected orientable compact subset of $\mathbf{R}^3$ which is a 3-manifold with boundary. Moreover, its boundary consists of finitely many components, each of which being a subset of the union of finitely many almost smooth surfaces. Motivated by numerical robustness issues, we consider a finite collection of boxes, with faces parallel to the coordinate planes, which covers the boundary of the solid. An interval solid is the union of this collection and the solid. In this paper we study the topology of a 3-manifold, when its boundary is covered by such a collection of boxes. We develop sufficient conditions on the collection of the boxes and the manifold, so that the union of the collection and the manifold is homeomorphic to the manifold itself. In particular, we apply this procedure to a solid and the associated interval solid. Finally, we present a method of constructing an interval solid, using interval arithmetic, homeomorphic to the solid.

Keywords: *robustness, approximate equality, solid modeling, data exchange, CAD model defects.*

1 Introduction

Building ideal boundary representation (B-rep) models of solids still remains beyond the reach of current computing technology, because most geometries in solid modeling cannot be represented exactly due to the precision limitation of the computer [2, 3]. In addition, pathological behaviors of geometric algorithms (particularly, geometric approximations) introduce significant computational errors. Together with round-off errors in numerical computations, such errors make topological decisions inconsistent, especially when geometric degeneracies occur. In boundary model representations, these errors leave gaps along edges and thus create inconsistency between topological and geometric information.

One solution widely adopted by CAD/CAM practice is the use of numerical or algorithmic tolerances. However, the semantics of such tolerancing and its influence on validity and topological properties of models have not been fully studied, although some aspects of this topic relating to data exchange are addressed in [1].

Research efforts have been mainly directed to develop new arithmetic systems in which numbers are representable in floating point and operations are closed. Essentially, these are approximation methods. Typical examples are integer and rational arithmetic (viewed here as approximations of real arithmetic), and interval and lazy arithmetic. See [4, 5, 6, 7, 8, 9, 10, 11, 12, 13] for some detailed descriptions.

As an efficient and powerful extension of traditional floating point representation, interval arithmetic and interval geometric representation not only increase numerical stability but

also assist in achieving model validity by defining gap-free boundaries. Hu et al [10, 11] introduced a method for robust solid modeling using interval arithmetic, and developed a data structure and Boolean operations for manifold and non-manifold interval boundary models. The required curve and surface intersection algorithms using interval arithmetic were presented in [14, 15]. However, topological issues involved in interval solid modeling were not studied in these papers [10, 11, 14, 15]. As an interval boundary model defines a family of infinitely many boundaries, maintaining topological invariance of such boundaries is, by no means, a trivial problem. This paper addresses such topological issues. Although the results presented here are primarily useful in boundary model reconstruction, they are also relevant in Boolean operations and boundary evaluation of interval models.

The paper is organized as follows: Section 2 studies the topology of the union of a collection of boxes which covers the boundary of a solid M. In particular, conditions on boxes are derived, so that the interval model constructed using such boxes defines a solid that is homeomorphic to M. Section 3 explains how such a collection of boxes can be constructed using interval surface intersection algorithms. Section 4 concludes the paper with a summary and identification of applications. The paper also includes an appendix which discusses construction of boxes guaranteed to contain a point on a B-spline surface, also needed in the developments of Section 3.

2 Covering Manifolds with Boxes

Throughout this paper, a *box* b refers to rectangular, closed parallepiped in $\mathbf{R}^3$ with positive volume, whose edges are parallel to the axes. A box defines a region in $\mathbf{R}^3$, and can be represented by an interval vector with nonzero components[1]. The size of a box is the maximum length of its edges. Operations on boxes using rounded interval arithmetic [16] preserve enclosure, meaning that the computed boxes always contain exact boxes under the same operations.

In this section, we present some results concerning the topology of a finite union of boxes. In particular, we shall be interested in the topology of a manifold when covered with boxes. The motivation behind this is our way of constructing interval models. See Section 3. We assume that the reader is familiar with the basic notions of topology [17]. Most of the terminology used here can be found in our earlier work [19].

Definition 2.1 *Let* $\mathcal{B}$ *be a* finite *collection of boxes, and let* $A \subseteq \mathbf{R}^3$. *We define* $\mathbf{B} = \cup\{b | b \in \mathcal{B}\}$ *and* $A^{\mathcal{B}} = A \cup \mathbf{B}$.

We begin with a general result. Let $\mathcal{B}$ be as above so that the following condition is satisfied:

A. Let $b_i, b_j \in \mathcal{B}$. Whenever $b_i \cap b_j \neq \emptyset$, then $b_{ij} = b_i \cap b_j$ is a box.

Then we have,

[1] An interval vector is a vector whose components are interval numbers.

Proposition 2.1 *Let the collection $\mathcal{B}$ satisfy condition* **A**. *Then,* **B** *is a compact 3-manifold with boundary.*

Proof: Without loss of generality, we may assume that $\mathcal{B}$ is *minimal* in the sense that $\mathbf{B} \neq \cup\{b \,|\, b \in \mathcal{B}, b \neq \beta\}$, for any $\beta \in \mathcal{B}$. Now notice that **B** is a compact subset of $\mathbf{R}^3$, since it is the union of a finite number of compact boxes. Moreover, we see that $\bigcup_{b_i \in \mathcal{B}}\{Int(b_i)\}$ is the interior of **B**.

We first observe that the boundary of **B**, $Bd(\mathbf{B}) = \mathbf{B} - Int(\mathbf{B})$, is non-empty, since **B** is compact. Evidently, the boundary of **B** consists of pieces from the boundaries of boxes. In fact, the boundary of every box b contains a piece of $Bd(\mathbf{B})$. For, if $q \in Bd(b)$ belongs to the interior of **B**, then q is in the interior of some box b_j. Since $\mathcal{B}$ is minimal, not all points of $Bd(b)$ are interior points of **B**, for otherwise, the removal of b would not alter **B**.

Let then $p \in Bd(\mathbf{B})$, and let $B_p = \{b \in \mathcal{B} \,|\, p \in b\}$. Obviously, $p \in Bd(b)$ for every $b \in B_p$. To simplify the notation, we may assume, after a translation, that p is the origin. We are going to show that near p, **B** has a 3D neighborhood homeomorphic to a halfspace. For $r > 0$, let $C = [-r, r]^3$. Denote by C_1, C_2, C_3, C_4 the intersection of C with the first four octants that are above the xy plane, and by C_5, C_6, C_7, C_8 the cubes symmetric to C_1, C_2, C_3, C_4 with respect to the xy-plane, respectively. We may pick r small enough so that: (a) no C_i intersects any element of $\mathcal{B} - B_p$, and (b) whenever C_i intersects the interior of a box b, then $C_i \subset b$. Now, we consider the possible non-manifold configurations of the set **B** *near* p, using the cubes C_i. **B** can be one of the following:

1. Either $C_{ij} = \cup_i C_i$, where there exist $i \neq j$ so that $C_i \cap C_j$ is equal to an edge l shared only by C_i and C_j, or its complement $C - C_{ij}$.

2. Either $D_{ij} = \cup_i C_i$, where there exist $i \neq j$ so that $C_i \cap C_j = \{p\}$ and p is shared only by C_i and C_j, or its complement $C - D_{ij}$.

We shall now prove that none of the above cases can happen.

1. Suppose that C_i, C_j share the edge l, which in turn is not shared by any other of the $C'_k s$. Then, from (b) above, there exist boxes b_i, b_j so that $C_i \subset b_i, C_j \subset b_j$. Let $b_{ij} = b_i \cap b_j$. Since $p \in Bd(\mathbf{B})$, l is part of an edge of b_{ij}. But since b_{ij} is nondegenerate from $\mathbf{A}$, l, by the above construction of the $C'_m s$, is also shared by another one of the $C'_k s$, a contradiction. The proof of case 2. is similar to the above. ■

Notice in the above that the boundary of $\mathbf{B}$ consists of pieces of planar surfaces.

Recall from [19] that a solid M is a (non-empty) connected compact orientable subset of $\mathbf{R}^3$ which is a 3-manifold with boundary ∂M. Moreover, ∂M consists of finitely many components, each of which is a subset of the union of finitely many almost smooth (AS)[2] surfaces R_i. The following is an immediate application of the previous result.

Corollary 2.1 *In case where* $\mathbf{B}$ *is connected, then* $\mathbf{B}$ *is a solid.*

Now let $V \subset \mathbf{R}^3$ be a compact connected orientable 2-manifold without boundary, and $\mathcal{B}$ as above. Suppose that, in addition to condition $\mathbf{A}$, $\mathcal{B}$ satisfies the following:

[2]A differentiable surface $\Phi \subset \mathbf{R}^3$ is smooth at a point (u_0, v_0, w_0) if there is a tangent plane to Φ at (u_0, v_0, w_0). We also call Φ an almost smooth (AS) surface if Φ is smooth for all points in its domain, except at a set of points of measure zero.

B1. $V \subset \mathbf{B}$, that is, $\mathcal{B}$ covers V, and

B2. $b \cap V \neq \emptyset$, for every $b \in \mathcal{B}$.

Recall, from Definition 2.1, that $V^{\mathcal{B}} = V \cup \mathbf{B} = \mathbf{B}$. It is easy to see that $V^{\mathcal{B}}$ is path connected. Indeed, let $u, v \in V^{\mathcal{B}}$. Then, $u \in b_1$ and $v \in b_2$, for some $b_1, b_2 \in \mathcal{B}$. Pick points $u_1 \in b_1 \cap V$ and $v_1 \in b_2 \cap V$. Since b_1, b_2 and V are (path) connected, there is a path in $V^{\mathcal{B}}$ that joins u and v. Thus, the above corollary gives us:

Corollary 2.2 *For $\mathcal{B}$ and $V^{\mathcal{B}}$ as above, $V^{\mathcal{B}}$ is a solid.*

If V is as above, the General Separation Theorem, [18], p. 179, asserts that its complement has precisely two connected components, V_I, V_O; we may assume that V_I is bounded and V_O unbounded. An argument similar to the one used in the proof of Proposition 2.1 shows that

Remark 2.1 *Let $\mathcal{B}$ be a finite collection of boxes that satisfies conditions* **A**, **B1** *and* **B2**. *Then, $V_I^{\mathcal{B}} = V_I \cup \mathbf{B}$ is a solid.*

Evidently, the above construction can be applied to solids as well. Indeed, if M is a solid, and $\mathcal{B}$ satisfies conditions **A, B1** and **B2** when V is replaced by C_i, where C_i is a connected componenet of ∂M, then the above result shows that $M^{\mathcal{B}} = M \cup \mathbf{B}$ is a solid. In that case we shall call $M^{\mathcal{B}}$ the *interval solid* generated by M and $\mathcal{B}$. Figure 1(c) shows a 2D example of such an $M^{\mathcal{B}}$. We shall see in the next section that such a solid can be constructed using interval surface intersection algorithms [14, 15].

A first step in this construction is the following set of conditions on $\mathcal{B}$ and V. The conditions are the following (see Figure 2):

C1. $\{Int(b_i),\ b_i \in \mathcal{B}\}$ is a cover of V.

C2. Each member b of $\mathcal{B}$ intersects V generically; that is, $b \cap V$ is a (closed) disk that separates b into two (closed) balls, B_b^+ and B_b^-, with $B_b^+, (B_b^-)$ lying in V_O (V_I), respectively.

C3. Whenever $b_i \cap b_j \neq \emptyset$, then $b_{ij} = b_i \cap b_j$ is a box that satisfies **C2**, for $b_i, b_j \in \mathcal{B}$.

Notice that the conditions **C1** and **C3** are similar in nature to **B1** and **A**. Condition **C2**, on the other hand, says that: (1) every b intersects V nicely, and (2) that V is a "locally flat" manifold; that is, every point in V has a neighborhood U in $\mathbf{R}^3$ so that $(U, U \cap V)$ is *homeomorphic* to $(\mathbf{R}^3, \mathbf{R}^2)$.

Consider now $S = V \cup V_I$. We will show that S is homeomorphic to $V_I^{\mathcal{B}} = V_I \cup \mathbf{B}$. To achieve that, we first need a technical lemma. We begin with some notation. Let $R = [a_1, a_2] \times [c_1, c_2], a_1 < a_2, c_1 < c_2$ be a square and let $P = [x_1, x_2] \times [y_1, y_2] \times [r, r], x_1 < x_2, y_1 < y_2, r > 0$ be such that $[x_1, x_2] \times [y_1, y_2] \in Int(R)$. Call the convex hull of the set of vertices of R and P a "g-trapezoid". Let $\mathcal{T}$ be a finite collection of g-trapezoids so that their union $\mathbf{T}{=}\cup\mathcal{T}$ is a 3-manifold with boundary. Let also the half space $Z = \{(x, y, z) \mid z \leq 0\}$. Then, evidently $Z \cup \mathbf{T}$ is a connected 3-manifold with boundary. Moreover, we have:

Lemma 2.3 *If $\mathcal{T}, Z$ as above, then*

1. *$Z \cup \mathbf{T}$ is homeomorphic to Z, and*

2. *The boundary of $Z \cup \mathbf{T}$ is homeomorphic to $\mathbf{R}^2$.*

Proof: 2. Let $p(x, y, z) = (x, y)$ be the projection map restricted to the boundary of $Z \cup \mathbf{T}$. Then, it is easy to see that p is a homeomorphism.

1. Let $\mathcal{T}'$ be the mirror image of the collection $\mathcal{T}$ with respect to the xy-plane, and let $\mathbf{T}'$ be the union of the elements of $\mathcal{T}'$. Let $q \in \mathbf{T}'$, and let L_q be the line that goes through q and is parallel to the z-axis. By 2., L_q intesects the boundary of $Z \cup \mathbf{T}$ at precisely one point, say Q'. Let Q'' be the point symmetric to Q' with respect to the xy-plane. Define the point $q' = q + \vec{Q''q}$. Now, define the map $g : \mathbf{T}' \to \mathbf{T}' \cup \mathbf{T}$ by $g(q) = q'$. Notice that g maps the vertical segment $[Q'', Q]$ to $[Q'', Q']$ in an 1-1 and onto fashion. Moreover, $g(Q'') = Q''$. Thus, g is a homeomorphism whose fixed points are precisely those points of the boundary of $\mathbf{T}'$ that lie strictly below the xy-plane. Finally, define

$$f : Z \to Z \cup \mathbf{T}, \qquad f(q) = \begin{cases} q' & \text{if} \quad q \in \mathbf{T}' \\ q & \text{otherwise} \end{cases}$$

Then, f is easily seen to be a homeomorphism. ■

The above shows that when a g-trapezoid t is removed (unglued) from $Z \cup \mathbf{T}$, the topology of the resulting manifold remains unchanged.

The above gives us the following:

Remark 2.2 *If $b \in \mathcal{B}$, then $S \cup b$ is homeomorphic to S.*

Proof: Consider the disk $D = b \cap V$. From **C2** we see that D separates b into two balls B_b^+ and B_b^-, with B_b^+ lying in the exterior of S while B_b^- lies in its interior. By "flattening" the disk D and imitating the proof of the above lemma, we see that we can find a homeomorphism $f : B_b^- \to b$ so that the following is satisfied: $f(x) = x$ for $x \in \partial B_b^- - Int(D)$ Finally, if $g : S \to S \cup b$ is defined by:

$$g(x) = \begin{cases} x & \text{if} \quad x \in S - B_b^- \\ \\ f(x) & \text{if} \quad x \in B_b^- \end{cases} \tag{1}$$

then, g is easily seen to be a homeomorphism. ■

We are now in a position to show the following:

Lemma 2.4 *S is homeomorphic to $V_I^{\mathcal{B}}$.*

Proof: The proof will be by induction on the number of elements of $\mathcal{B}$. Remark 2.2 provides the first step in the induction procedure. Let us then consider a subcollection $\mathcal{B}_1$ of $\mathcal{B}$ having more than one element, and let $S_1 = S \cup \mathbf{B}_1$. Take an element $b \in \mathcal{B}_1$, and consider the disk $\Delta = V \cap b$. By flattening the disk Δ and invoking Lemma 2.3, as well as condition **C3**, we see that near Δ, S_1 looks like the halfspace Z with a g-trapezoid t attached to it. But then, when t is removed, the topology of S_1 near Δ remains the same, and thus $S \cup \mathbf{B}_1$ is homeomorphic to $S \cup \mathbf{B}_2$, where $\mathcal{B}_2 = \mathcal{B}_1 - \{b\}$. By induction, that

means that S is homeomorphic to $S \cup \mathbf{B}_1$. ■

Now we are ready to state the main result of this section. Let M be a compact connected 3-manifold with boundary, and let $\mathcal{B}$ be a finite collection of boxes in $\mathbf{R}^3$ that satisfies conditions **C1-C3**, when V is replaced by ∂M. Then we have:

Theorem 2.5 *Let M, $\mathcal{B}$ be as above. Recall that $M^{\mathcal{B}} = M \cup \mathbf{B}$. Then, $M^{\mathcal{B}}$ is a 3-manifold homeomorphic to M. In fact, $M^{\mathcal{B}}$ is a solid.*

Proof: Since M is compact, its boundary ∂M consists of finitely many components, say $C_1, C_2, \cdots, C_k$. If b is in $\mathcal{B}$, notice from **C2** that b intersects *only* one component of ∂M. Then, for $1 \leq i \leq k$, define $\mathcal{B}_i$ to be the collection of boxes that intersect C_i. In that case Lemma 2.4 shows that $M \cup \mathbf{B}_i$ is homeomorphic to M, for each i. Finally, using induction on the number of components of ∂M, Lemma 2.4 and Remark 2.1, we complete the proof.

■

Corollary 2.6 *If M is a solid and $\mathcal{B}$ satisfies conditions* **C1** *through* **C3**, *then $M^{\mathcal{B}}$ and $M - \mathbf{B}$ are interval solids that are homeomorphic to M.*

Observe that in Corollary 2.6 condition **C1** is very natural in order for $M^{\mathcal{B}}$ to be an interval solid. The fact that $\mathcal{B}$ has to satisfy **C2** says that for every connected component C_i of ∂M, every member of $\mathcal{B}_i$ has to be in an open neighborhood N_i of C_i, and these N_i's are mutually disjoint. The latter puts a constraint on how big the boxes can be. In fact, we may confine each member of $\mathcal{B}_i$ to be in a *tubular neighborhood* T_i of C_i. Condition **C3**

puts some constraints on the structure of $\mathcal{B}$. In the next section we shall show how such a collection can be constructed by using interval surface intersection (ISI) algorithms (e.g. [15]) with sufficiently tight resolution.

We close this section with the following definition which is motivated by the above results:

Definition 2.2 *Let M be a solid, and $\mathcal{B}$ be a finite collection of boxes. We say that the interval solid $M^{\mathcal{B}}$ is* approximately equal *to M if $M^{\mathcal{B}}$, as well as $M - \mathbf{B}$, are homeomorphic to M.*

Figure 1 gives an example of an $M^{\mathcal{B}}$ which is approximately equal to M.

3 Construction of interval solids

The aim of this section is the construction of interval solids approximately equal to a solid using methods of interval arithmetic.

The size of a box, in general, has little influence on approximate equality. The example in Figure 3(a) illustrates that no matter how small the sizes are, approximate equality may not be achievable; on the other hand, Figure 3(b) shows that the sizes could be fairly large while still maintaining approximate equality. As discussed in the previous section, it is the *structure* of boxes that determines the property of approximate equality. However, boxes constructed by evaluating surfaces and computing their intersections using interval arithmetic, have certain properties which guarantee that a sufficiently tight resolution ε

exists such that the conditions **C1**–**C3** are all satisfied if the box sizes are no larger than ε.

The appendix shows that boxes evaluated on a B-spline surface have centers on the exact surface and their sizes are piecewise monotonous over the parameter domain. In the following, we illustrate that interval models constructed using an ISI algorithm have, in general, the property of approximate equality. The ISI algorithm used in our work is described in Hu et al [15].

In an interval model generated from a solid M, we call boxes that cover only the interiors of faces *face boxes*, i.e. face boxes do not intersect edges and vertices. A face box can be constructed by evaluating an interval point in the interior of a region bounded by a collection of rectangles in the parameter domain of the underlying surface. These rectangles are solutions of surface intersections using an ISI algorithm, and their union contains the pre-images of edges and vertices in the parameter domain. See Figure 4 for an example. As an intersection curve computed by an ISI algorithm is an ordered list of boxes, the intersection of two such curves is a cluster of boxes whose union contains the exact intersection point. If this point happens to be an vertex, the boxes in the cluster are called *vertex boxes*. Boxes between two clusters of vertex boxes on an intersection curve, are called *edge boxes*. Notice that an edge box only covers a piece of an edge but none of vertices. See also Figure 4 for examples of edge box and vertex box. Because boxes computed using an ISI algorithm always contain exact surface intersections, such a collection of boxes is guaranteed to cover the exact boundary ∂M so that **C1** is satisfied.

Now note that the topology of $\mathbf{R}^n$ remains the same when one replaces "open balls" with "open boxes". Since ∂M is a 2-manifold without boundary, for each point $p \in \partial M$, there exists a box b that contains p so that $Int(b) \cap \partial M$ is an open disk, as well as $b \cap \partial M$ is a closed disk.

Let b be a face box, because its center is a point in ∂M, $b \cap \partial M$ is a closed disk for sufficiently small box size. If b is an edge box, it is an intersection box of two surfaces. Assume that the exact solution for one intersection point is $\{u, v\}$ and $\{s, t\}$ in the parameter domains. Due to the use of rounded interval arithmetic, the interval solution is $([u^l, u^u], [v^l, v^u])$ and $([s^l, s^u], [t^l, t^u])$ such that $u \in (u^l, u^u), v \in (v^l, v^u), s \in (s^l, s^u)$ and $t \in (t^l, t^u)$. Therefore, the interior of b also contains at least one point in ∂M. When the box size is sufficiently small, **C2** is satisfied. For a vertex box, the same argument holds.

In general, **C3** is satisfied. Exceptions happen when boxes intersect 1) at the positions of the global minimum self-distance; 2) due to the variation of box size. See Figure 5(a); 3) due to small geometric features. See Figure 5(b); 4) at a lower dimensional entity. At a given resolution, indeed, case 1 and 2 will be detected by an ISI algorithm as surface intersections. As the resolution increases, in both cases overlapping boxes will eventually become disjoint. For example, if the maximum box size is less than $d/\sqrt{3}$, where d is the minimum self-distance, case 1 will never happen[3]. Case 4 can be eliminated by slightly reducing or increasing the size of one box while maintaining its relations with other boxes.

[3]This is because the circumscribed spheres of any two boxes do not intersect due to the minimum self-distance.

For case 3, we have the following remark:

Remark 3.1 *If $b_{ij} \cap V = \emptyset$ in* **C3***, then, Lemma 2.4 holds if there exists a subcollection $\mathcal{B}_k$ such that 1) $\mathbf{B}_k = \cup\{b|b \in \mathcal{B}_k\}$ is a closed ball satisfying* **C2***; 2) $\mathbf{B}_k \cap b_{ij}$ is also a closed ball, and 3) $\mathbf{B}_k \cap b_i$ and $\mathbf{B}_k \cap b_j$ satisfy* **C3***.*

This is because b_i, b_j and $\mathcal{B}_k$ can be replaced by closed balls satisfying **C3**. For example, in Figure 6, b_i, b_j and b_k can be replaced by $b_i' = b_i - b_{k1}, b_j' = b_j - b_{k1}$ and $b_k' = b_k \cup b_{k2}$, where $b_{ij} \subset b_{k1} \subset b_{k2}$ and $b_{k1} \cap V = \emptyset, b_{k2} \cap V = \emptyset$.

In the following, we study how to construct 2D boxes satisfying the conditions in Remark 3.1. The discussion serves as an explanation of the existence of such a box collection, rather than a computation method.

Let b_1, b_2 be two boxes evaluated on the same B-spline curve C and $(b_1 \cap b_2) \cap C = \emptyset$. Denote the half-widths of a 2D box by $(\varepsilon_x, \varepsilon_y)$. See the example in Figure 7. Assume that $\varepsilon_{y1} \leq \varepsilon_{y2}$ and the half-width of boxes between b_1 and b_2 varies monotonously. Observe that if the curve segment $\widehat{c_1c_2} - (\widehat{c_1c_2} \cap (b_1 \cup b_2))$, where c_1, c_2 are the centers, is above line $l : y = c_{y2} - (\varepsilon_{y1} + \varepsilon_{y2})$, then, boxes covering $\widehat{c_1c_2}$ forms a closed ball satisfying the conditions in Remark 3.1. A sufficient condition for this to happen is that the part of C between c_1 and c_2 lies inside the circle which passes through c_1, c_2 and intersects line l at point p with the condition that p is the intersection point with the larger x-coordinate, where p is the intersection point of line l and the right edge of b_1. See Figure 7(a). If p does not exist as shown in Figure 7(b), the circle should pass through c_1, c_2 and tangent to line l.

Without loss of generality, assume that c_1 is the origin. Then, the radius of the said circle, r depends on the position of c_2 and the half-widths, i.e.

$$r = \psi(c_{x2}, c_{y2}, \varepsilon_{x1}, \varepsilon_{y1}, \varepsilon_{x2}, \varepsilon_{y2}), \tag{2}$$

with

$$\begin{aligned} c_{x2} &\in [0, \varepsilon_{x1} + \varepsilon_{x2}], \\ c_{y2} &\in [0, \varepsilon_{y1} + \varepsilon_{y2}], \end{aligned}$$

such that $b_1 \cap b_2 \neq \emptyset$. Let ε_t be the resolution in the parameter domain of curve C. The half-widths of boxes are bounded in $[\varepsilon_x^l, \varepsilon_x^u]$ and $[\varepsilon_y^l, \varepsilon_y^u]$, where the bounds can be computed using Eq. (13) in the appendix with $\varepsilon = \frac{1}{2}\varepsilon_t$. The overall maximum radius is thus

$$\begin{aligned} R_{max} &= \max(\psi(c_{x2}, c_{y2}, \varepsilon_{x1}, \varepsilon_{y1}, \varepsilon_{x2}, \varepsilon_{y2})), \\ c_{x2} &\in [0, 2\varepsilon_x^u], \\ c_{y2} &\in [0, 2\varepsilon_y^u], \\ \varepsilon_{x1}, \varepsilon_{x2} &\in [\varepsilon_x^l, \varepsilon_x^u], \\ \varepsilon_{y1}, \varepsilon_{y2} &\in [\varepsilon_y^l, \varepsilon_y^u].. \end{aligned} \tag{3}$$

Thus, the conditions in Remark 3.1 will be satisfied if

$$R_{max} \leq R_{\kappa}. \tag{4}$$

In summary, for a sufficiently tight resolution, boxes constructed using an ISI algorithm form an interval solid which is approximately equal to the exact solid.

4 Conclusion

In Hu et al [10, 11] the concept of an interval solid model was first introduced and methods for its construction were presented. Moreover, the issue of topological equivalence of a solid and its associated interval solid was recognized, but not fully resolved. This paper provides a set of sufficient conditions on the collection of boxes as well as the solid's boundary which guarantee this equivalence. In doing so, we introduced the notion of approximate equality between a solid and its associated interval solid. We also provide a procedure for constructing interval solid models in the case where the boundary of the solid consists of B-spline patches. The theoretical results of this paper are used in [20, 21, 22] to provide methods for verifying the geometric consistency of B-rep models and evaluate existing inconsistencies using interval solids. In those papers we also convert B-rep models into interval solid models in order to rectify them. In addition, examples are provided to illustrate the above concepts and procedures. Methods for verifying the above topological

equivalence are expected to be time consuming because of the plethora of boxes involved in actual models and the complexity of the rectification process itself. Future research should focus on making the above procedures more efficient in order to help realize the potential of interval solid modeling methods in resolving the long standing robustness problem in solid modeling.

Appendix: Boxes on B-spline surfaces

Evaluation of a B-spline surface $P(t)$ at a certain parameter value t_0 using interval arithmetic creates a box guaranteed to containing $P(t_0)$. In the following, we study the location and size of such boxes. For detailed description of interval arithmetic and interval B-splines, see [23, 24].

An interval number $[X]$ represents an interval $[X^l, X^u]$, where X^l and X^u are the lower and upper bounds. The center of $[X]$ is $X_c = \frac{1}{2}(X^l + X^u)$, and the width is $w([X]) = X^u - X^l$. Thus, $[X] = X_c + \frac{1}{2}w([X])[I]$, where $[I] = [-1, 1]$.

Let $[D_i]$ be the control points of a B-spline function, $\{t_i\}$ be the knot vector. Let $[t] = t + \varepsilon[I]$ be an interval parameter, where ε is the half-width of $[t]$. The recursive formula of de Boor's algorithm is

$$[D_i^j] = (1 - [\alpha_i^j])[D_{i-1}^{j-1}] + [\alpha_i^j][D_i^{j-1}], \tag{5}$$

where

$$[D_{i-1}^{j-1}] = D_{i-1}^{j-1} + h_{i-1}^{j-1}[I], \tag{6}$$

$$[D_{i}^{j-1}] = D_{i}^{j-1} + h_{i}^{j-1}[I], \tag{7}$$

with $[D_i^0] = [D_i], h_i^0 = \frac{1}{2}w([D_i])$, and

$$[\alpha_i^j] = \frac{[t] - t_i}{t_{i+k-j} - t_i}. \tag{8}$$

By plugging $[t]$ in the formula, we have

$$\begin{aligned}[D_i^j] &= (1-\alpha_i^j)D_{i-1}^{j-1} + \alpha_i^j D_i^{j-1} \\ &\quad + \left((1-\alpha_i^j)h_{i-1}^{j-1} + \alpha_i^j h_i^{j-1} + (|D_i^{j-1}| + |D_{i-1}^{j-1}|)\Delta t_i^j + (h_i^{j-1} + h_{i-1}^{j-1})\Delta t_i^j\right)[I], \end{aligned} \tag{9}$$

where

$$\alpha_i^j = \frac{t - t_i}{t_{i+k-j} - t_i}, \tag{10}$$

$$\Delta t_i^j = \frac{\varepsilon}{t_{i+k-j} - t_i}. \tag{11}$$

Therefore, $[D_i^j]$ can be represented as $D_i^j + h_i^j[I]$ with

$$D_i^j = (1-\alpha_i^j)D_{i-1}^{j-1} + \alpha_i^j D_i^{j-1}, \tag{12}$$

$$h_i^j = (1-\alpha_i^j)h_{i-1}^{j-1} + \alpha_i^j h_i^{j-1} + (|D_i^{j-1}| + |D_{i-1}^{j-1}|)\Delta t_i^j + (h_i^{j-1} + h_{i-1}^{j-1})\Delta t_i^j. \quad (13)$$

Denote the function value as $[P([t])]$. Then, the center of $[t]$ maps to the center of $[P([t])]$. Note that Eq. (13) is a polynomial function of t in each span of the parameter domain, and therefore, the width of $[P([t])]$ varies piecewise monotonously. If a knot $t_i \in [t]$, $w([P([t])]) = w([P([t_1])]) + w([P([t_2])])$ where $[t_1] = [t] \cap [t_{i-1}, t_i]$ and $[t_2] = [t] \cap [t_i, t_{i+1}]$. In summary, a box evaluated on a surface has its center on the exact surface. The size in each axis direction varies piecewise monotonously.

Acknowledgments

Funding for this work was obtained in part from NSF grant DMI-9215411, ONR grant N00014-96-1-0857 and from the Kawasaki chair endowment at MIT. The authors would like to thank Dr. W. Cho and Dr. G. Yu for their assistance in the early phases of the CAD model rectification project, Professors Ronald Fintushel and Thomas Peters, and the referees of this manuscript for their helpful comments which led to an improvement of the paper.

References

[1] T. J. Peters, N. F. Stewart, D. R. Ferguson, P. S. Fussel, Algorithmic tolerances and semantics in data exchange, *Proceedings of the 13th ACM Symposium on Computational Geometry*, pp. 403–405, June 1997, Nice, France.

[2] C. M. Hoffmann, The problems of accuracy and robustness in geometric computation, *Computer*, 22(3):31–41, 1989.

[3] C. M. Hoffmann, *Geometric and Solid Modeling–An Introduction*, Morgan Kaufmann Publishers Inc., San Mateo CA, 1989.

[4] V. Milenkovic, Robust polygon modelling, *Computer Aided Design*, 25(9):546–566, 1993.

[5] S. Fortune, Polyhedral modeling with multiprecision integer arithmetic, *Computer Aided Design*, 29(2):123–133, 1997.

[6] J. Keyser, S. Krishnan and D. Manocha, Efficient and accurate B-rep generation of low degree sculptured solids using exact arithmetic: I–representations, *Computer Aided Geometric Design*, 16:841–859, 1999.

[7] J. Keyser, S. Krishnan and D. Manocha, Efficient and accurate B-rep generation of low degree sculptured solids using exact arithmetic: II–computation, *Computer Aided Geometric Design*, 16:861–882, 1999.

[8] D. Salesin, J. Stolfi and L. Guibas, Epsilon geometry: building robust algorithms from imprecise computations, in *Proceedings of the 5th ACM Annual Symposium on Computational Geometry*, Saarbruchen, West Germany, 1989, pp. 208-217.

[9] D. H. Salesin, *Epsilon Geometry: Building Robust Algorithms from Imprecise Computations*, Ph.D. thesis, Stanford University, 1991.

[10] C.-Y. Hu, N. M. Patrikalakis, and X. Ye, Robust interval solid modeling: part I, representations, *Computer Aided Design*, 28(10):807–817, 1996.

[11] C.-Y. Hu, N. M. Patrikalakis, and X. Ye, Robust interval solid modeling: part II, boundary evaluation, *Computer Aided Design*, 28(10):819–830, 1996.

[12] M. O. Benouamer, D. Michelucci and B. Peroche, Error-free boundary evaluation based on a lazy rational arithmetic: a detailed implementation, *Computer Aided Design*, 26(6):403–416, 1994.

[13] A. Agrawal, *A General Approach to the Design of Robust Algorithms for Geometric Modeling*, Ph.D. thesis, University of Southern California, 1995.

[14] C.-Y. Hu, T. Maekawa, E. C. Sherbrooke and N. M. Patrikalakis, Robust interval algorithm for curve intersections, *Computer Aided Design*, 28(6/7):495–506, 1996.

[15] C.-Y. Hu, T. Maekawa, N. M. Patrikalakis and X. Ye, Robust interval algorithm for surface intersections, *Computer Aided Design*, 29(9):617–627, 1997.

[16] S. L. Abrams, W. Cho, C.-Y. Hu, T. Maekawa, N. M. Patrikalakis, E. C. Sherbrooke and X. Ye, Efficient and reliable methods for rounded interval arithmetic, *Computer Aided Design*, 30(8):657–665, 1998.

[17] J. R. Munkres, *Topology: a first course*. Prentice Hall, Englewood Cliffs, New Jersey, 1975.

[18] M. Greenberg, *Lectures on Algebraic Topology*. W.A. Benjamin, Inc., New York, 1967.

[19] T. Sakkalis, G. Shen and N. M. Patrikalakis, Representational Validity of Boundary Representation Models. *Computer Aided Design*, 32(12):719–726, October 2000.

[20] G. Shen, T. Sakkalis and N. M. Patrikalakis, Interval Methods for B-Rep Model Verification and Rectification. *Proceedings of ASME 2000 IDETC/CIE, 2000 ASME Design Automation Conference*, Baltimore, MD, September 2000. p. 140 and CDROM. NY: ASME, 2000.

[21] G. Shen, T. Sakkalis and N. M. Patrikalakis, Manifold Boundary Representation Model Rectification. *Proceedings of the 3rd International Conference on Integrated Design and Manufacturing in Mechanical Engineering*, C. Mascle, C. Fortin, J. Pegna, editors. p. 199 and CDROM. Montreal, QC, Canada. May 2000. Presses internationales Polytechnique, Montreal, Canada, May 2000.

[22] N. M. Patrikalakis, T. Sakkalis and G. Shen, Boundary Representation Models: Validity and Rectification. *Proceedings of the 9th IMA Conference on the Mathematics*

of Surfaces, University of Cambridge, UK, September 2000. R. Cipolla and R. Martin, editors. pp. 389–409, London UK, Springer Verlag 2000.

[23] R. E. Moore, *Interval Analysis*. Prentice-Hall, Englewood Cliffs, NJ, 1966.

[24] G. Shen and N. M. Patrikalakis, Numerical and geometric properties of interval B-splines. *International Journal of Shape Modeling*, 4(1/2):35–62, 1998.

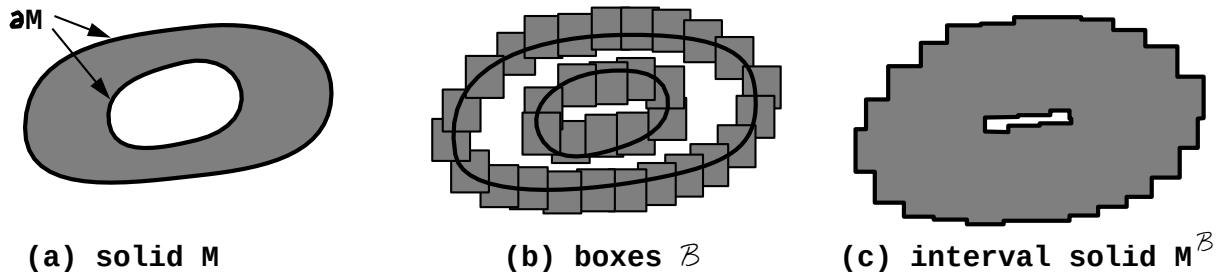

Figure 1: An example of interval solid

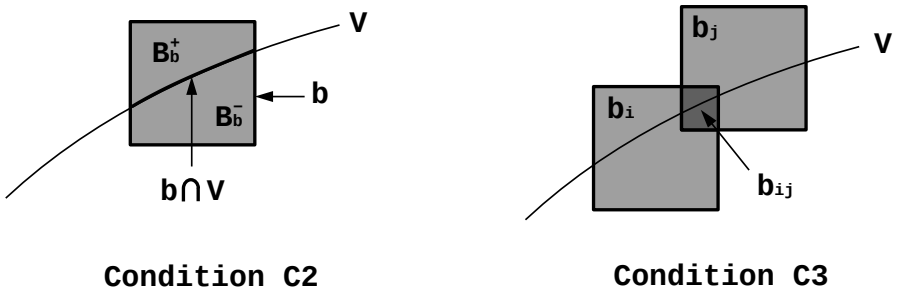

Figure 2: 2D version of condition **C2** and **C3**

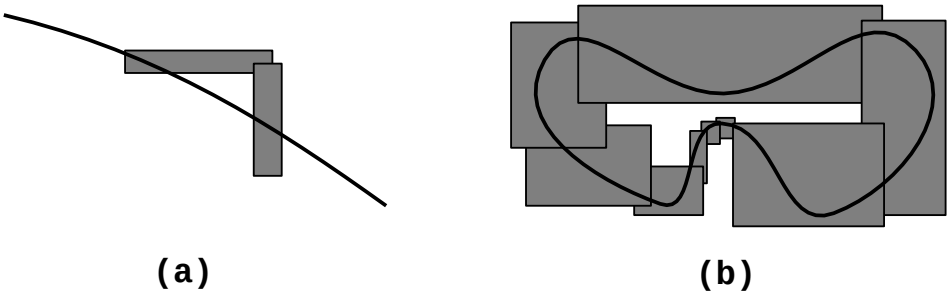

Figure 3: Influence of box sizes on approximate equality

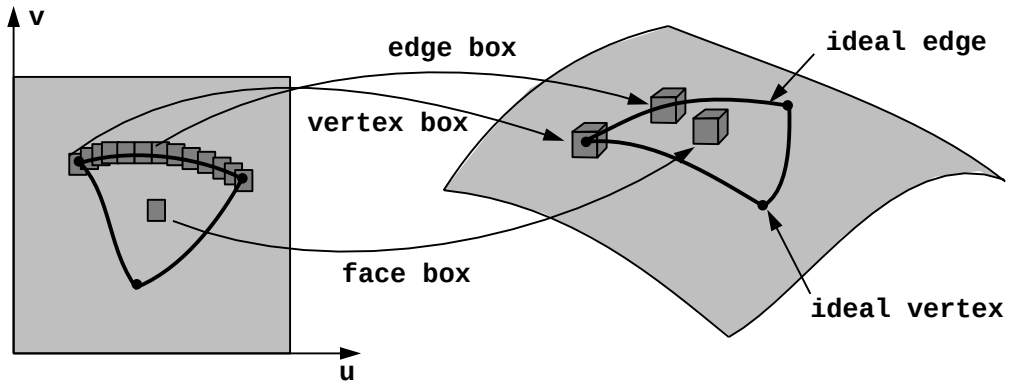

Figure 4: Boxes of an interval model

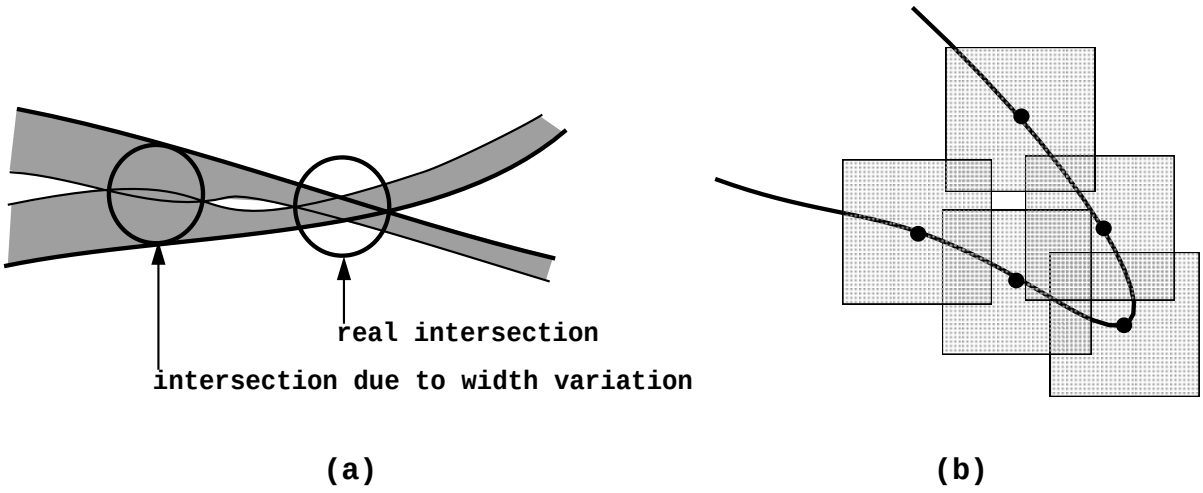

Figure 5: Exceptions to **C3**

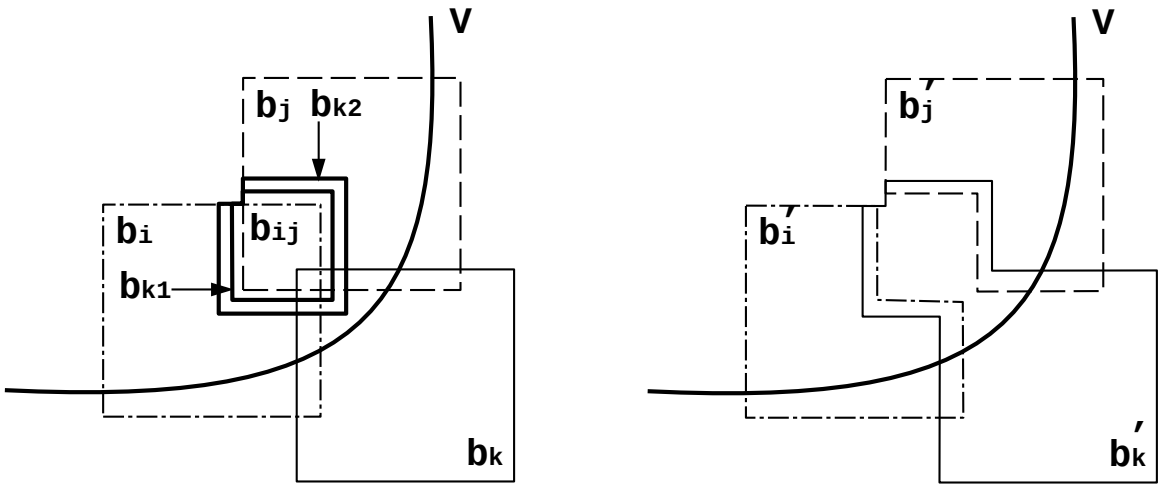

Figure 6: Illustration of Remark 3.1

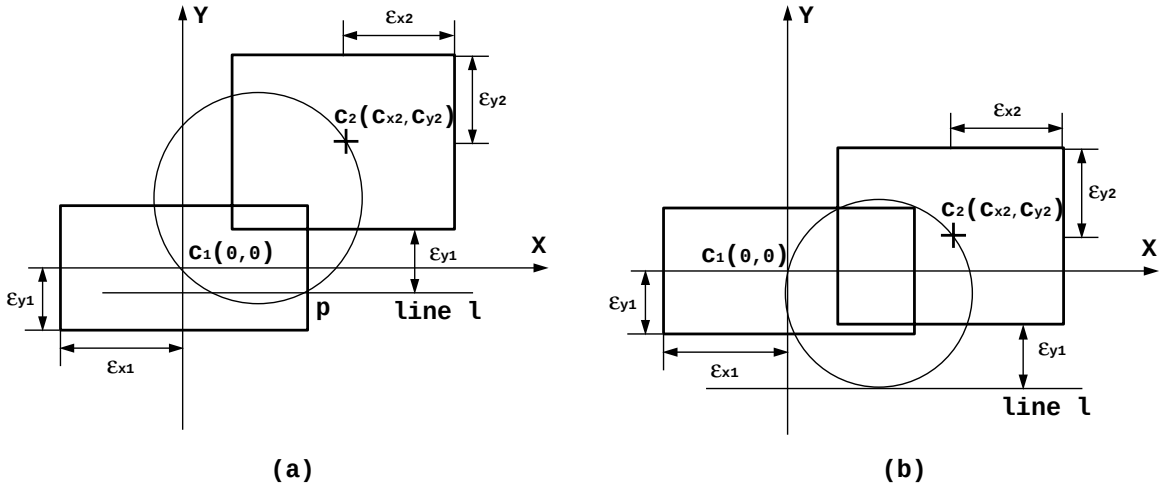

Figure 7: Construction of 2D boxes satisfying the conditions in Remark 3.1

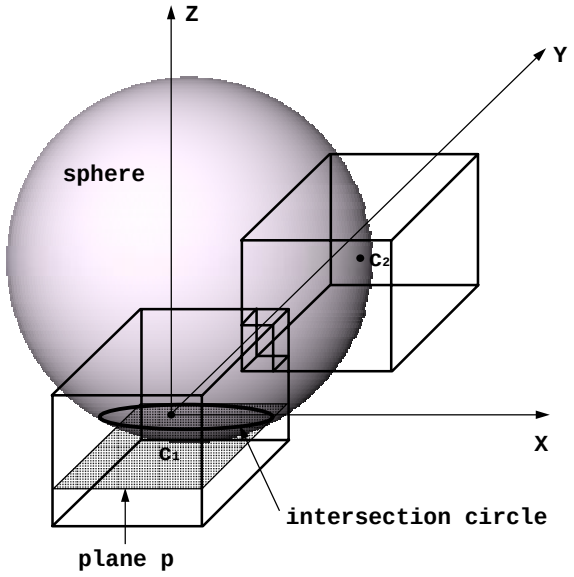

Figure 8: Construction of 3D boxes satisfying condition Remark 3.1